growth or Ostwald crystal growth occurs (or both overlap) remains to be further worked out. Our experimental results suggest that the Ostwald mechanism should be considered as only one possible approach to the formation of bulk materials.

Summary

A novel sol-gel synthesis of ZnO has been presented. The formation of ZnO crystals was followed spectroscopically throughout the transition from cluster to syrup to alcogel to crystal. Changes in the spectroscopic properties accompanying these transitions were explained in terms of aggregation. Although there are some uncertainties in fitting the data to quantum mechanical models, it seems that the physical idea of a Coulomb-based electron-hole attraction is as effective a model as it is simple. In addition, the presence of primary and secondary aggregate sizes suggests that membranes and films prepared from the ZnO particles would display primary and secondary pore size distributions. Q-ZnO colloids have been successfully applied in fabrication of thin epitaxial ZnO films and ceramic membranes. This will be the subject of another publication. We did not attempt to delve deeply into the complex field of crystal growth. The main purpose of this study is to encourage the use of luminescing semiconductor clusters and corresponding spectroscopic measurement techniques to study aggregation phenomena and crystal growth mechanisms.

Acknowledgment. We gratefully acknowledge the financial support from the NSF (Contract CES-8504276), the U.S. DOE (Contract DE-FC07-88ID12778), and SSI Technologies, Inc. (Janesville, WI). We express our gratitude to Dr. Walt Zeltner for helpful discussions. We enjoyed a very pleasant collaboration with Dr. Grayson Scott (Medical Sciences Department, UW—Madison) during the transmission electron microscopic studies and thank him for his help.

Registry No. ZnO, 1314-13-2; EtOH, 64-17-5.

Twisted Intramolecular Charge-Transfer Fluorescence of Aromatic Amides: Conformation of the Amide Bonds in the Excited States

Isao Azumaya,[†] Hiroyuki Kagechika,[†] Yoshihisa Fujiwara,[‡] Michiya Itoh,[‡] Kentaro Yamaguchi,[§] and Koichi Shudo*,[†]

Contribution from the Faculty of Pharmaceutical Sciences, University of Tokyo, 7-3-1 Hongo, Bunkyo-ku, Tokyo 113, Japan, Faculty of Pharmaceutical Sciences, Kanazawa University, Takara-machi, Kanazawa 920, Japan, and School of Pharmaceutical Sciences, Showa University, Hatanodai, Shinagawa-ku, Tokyo 142, Japan. *Received July 16, 1990*

Abstract: The mechanism of the dual fluorescences of benzanilide (**1**) and *N*-methylbenzanilide (**2**) in methylcyclohexane was investigated. The emission at longer wavelength is composed of one component for **1** (λ_{max} 477 nm) and of one major component (96%, λ_{max} 518 nm) for **2**. Various substitutions on the aromatic rings permit the study of the F_2 fluorescence wavelength and intensity on twisting about the Ar–CO, the Ar–N, and the amide bond (N–CO) itself. Though the ground-state structures of **1** and **2** are very different from each other, the structures of the emitting species of both compounds are considered to be similar. Studies on conformationally restricted derivatives showed that the amide bond must be rotated for the emission of longer wavelength. Quantitative data indicate that the F_2 emissions are generated from excited twisted intramolecular charge-transfer (TICT) species with twisted amide bonds.

Introduction

Benzanilide (**1**) exhibits an anomalous fluorescence with a large Stokes shift that is at longer wavelength than that of its phosphorescence.[1] Generally, such anomalous fluorescence is emitted from a species that is energetically much more stabilized than the primarily formed species. Recent nano- or picosecond studies on the large Stokes-shifted fluorescence have revealed various mechanisms, such as the formation of an intra- or intermolecular excited complex (excimer, exciplex, solvent reorientation, and so forth) or a change of the structure (proton transfer,[2] twisted intramolecular charge transfer,[3] and so forth). However, the emitting mechanism of aromatic anilides including benzanilide (**1**) has seemed to be complicated. In 1971, O'Connell et al. reported that the fluorescence of **1** was observed only in the solid state or in a rigid matrix of EPA (ethyl ether:isopentane:ethanol = 5:5:2 v/v).[1] Furthermore, *N*-phenylisoindolinone, which is a conformationally restricted analogue of **1** containing a five-membered ring system, was shown to emit similarly to **1** even at room temperature in fluid EPA. These results indicated that only quite subtle changes of geometry at the emitting states must be occurring. Recently, Tang et al.[4] and Heldt et al.[5,6] showed that the fluorescence at longer wavelength of **1** in cyclohexane or methylcyclohexane (MCH) could be ascribed to two overlapping mechanisms, that is, proton transfer and twisted intramolecular charge transfer (TICT), using dielectric solvent effects on spectral position, band half-width, and solvent environmental effects. They then sought to confirm these assignments by time-resolved absorption spectroscopy and fluorescence decay dynamics studies.[7] However, their conclusion on the emitting mechanisms was based in part on biexponential fitting of the fluorescence decay curve of **1** and a comparison with the fluorescence of *N*-methylbenz-

[†] University of Tokyo.
[‡] Kanazawa Univeristy.
[§] Showa University.

(1) O'Connell, E. J., Jr.; Delmauro, M.; Irwin, J. *Photochem. Photobiol.* **1971**, *14*, 189–195.
(2) See special issue of "Spectroscopy and dynamics of elementary proton transfer in polyatomic systems": *Chem. Phys.* **1989**, *136*, 153–360.
(3) Rettig, W. *Angew, Chem., Int. Ed. Engl.* **1986**, *25*, 971–988.
(4) Tang, G.-Q.; MacInnis, J. M.; Kasha, M. *J. Am. Chem. Soc.* **1987**, *109*, 2531–2533.
(5) Heldt, J.; Gormin, D.; Kasha, M. *J. Am. Chem. Soc.* **1988**, *110*, 8255–8256.
(6) Heldt, J.; Kasha, M. *J. Mol. Liq.* **1989**, *41*, 305–313.
(7) Heldt, J.; Gormin, D.; Kasha, M. *Chem. Phys.* **1989**, *136*, 321–334.

0002-7863/91/1513-2833$02.50/0

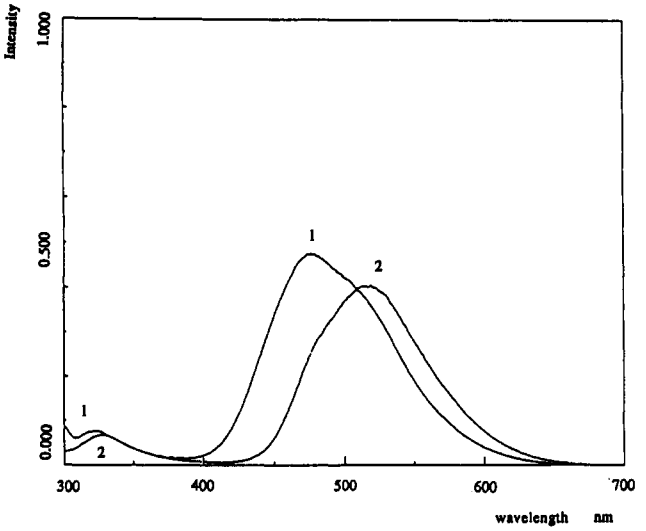

Figure 1. Fluorescence spectra of **1** (2.7×10^{-5} M) and **2** (3.4×10^{-5} M) in MCH at 300 K. Each spectrum was obtained by excitation at the excitation maximum wavelength as shown in Table I.

anilide (**2**), which has no acidic protons and therefore has a single decay constant. They did not consider the experimental ground-state structures of these compounds.

Our systematic investigations on the physicochemical and biological properties of aromatic anilides have shown that the character of the amide bond is sensitively affected by substitution or by environmental conditions. Most significantly, N-methylation of secondary anilides results in the stabilization of the cis conformation.[8-10] Further, the steric and electronic effects of the substituents on the aromatic ring change the stabilities of the conformers with a trans or cis amide bond, their rotational barriers, and so on.[11] In this study, the steady-state fluorescence and picosecond decay dynamics of a series of aromatic anilides were investigated. The results revealed twisting of their amide bonds at the excited states in nonpolar solvents.

Results and Discussion

Dual Peaks of Fluorescence of Benzanilide and *N*-Methylbenzanilide. Figure 1 shows the fluorescence spectra of benzanilide (**1**) and *N*-methylbenzanilide (**2**) in methylcyclohexane (MCH) at room temperature. As reported before, each compound exhibits anomalous dual peaks of fluorescence, one in the normal region (F_1 emission) for such aromatic compounds and the other shifted to a longer wavelength (F_2 emission). Since the intensities of F_1 emissions of both compounds increased with time, the observed F_1 emissions seem to be mixed emissions from the anilides and their photodegraded products.[4]

The maximum wavelength of F_2 emission was not affected by the concentration of anilides below 3×10^{-4} M for **1** (λ_{max} 477 nm) and below 3×10^{-3} M for **2** (λ_{max} 518 nm). The fluorescence intensity at the maximum wavelength was proportional to concentration below 1×10^{-4} M for **1** and 3×10^{-4} M for **2**, but not at higher concentrations. Similarly, the maximum wavelengths of the excitation spectra were strongly red-shifted above these high concentrations (Figure 2). One possible reason is that the polarity of the solution increases as the concentration of anilides is increased. Indeed, F_2 emissions were observed strongly in nonpolar solvents such as MCH, *n*-hexane, and CCl_4 and weakly in polar solvents (THF, methanol, and $CHCl_3$).

The fluorescence decay curves for F_2 emissions of both anilides (**1** and **2**) were obtained in MCH at 300 K as shown in Figure 3. Compound **1** exhibits a single exponential curve with a decay time of 860 ps. The decay curve for **2** consisted of essentially one component with a decay time of 1.65 ns, though the best biexponential fit was obtained by adding 4% of a slow component (16.5 ns). The same values were obtained for the sample after several recrystallizations, and so the minor component was not the emission from an impurity. Heldt et al. reported that F_2 emission of **1** in cyclohexane at 298 K consisted of two overlapping peaks of fluorescence, 78% of a short lifetime component (0.77 ns), and 22% of a long lifetime component (1.45 ns).[7] From the decay curve of **2** with a single-exponential fit (1.45 ns), they concluded that the former is the fluorescence from the imidol tautomer produced by double proton transfer in the hydrogen-bonded dimer of *cis*-benzanilide, i.e., it is peculiar to **1**, and the later is TICT emission that is common to both anilides. Though these results on the decay dynamics seem plausible at first sight, they also pointed out that the exponential fit by a single component is better and therefore suggested the possibility of one-component fluorescence (870 ps) for F_2 emission of **1**, which is consistent with our result. The ambiguity of their interpretation of the decay dynamics would have been caused by the fitting on a linear scale. Indeed, we ascertained that the decay curve of **1** could be fitted superficially with either one component or two components on a linear scale. However, the fitting on a logarithmic scale definetly excludes the two-component decay of fluorescence of **2**. Thus,

Table I. Trans to Cis Ratios of the Aromatic Anilides in Solution and Their F_2 Fluorescence Data in MCH at 300 K

	trans:cis ratio[a]			F_2 emission		
compd	$CDCl_3$	C_6D_{12}	CCl_4	λ_{max} (nm)	rel intens	excitation λ_{max} (nm)
1	100:0			477	1.00	271
3	100:0			480	0.48	269
4	97:3			479	0.12	258
5	100:0			482	1.08	272
6	100:0			509	0.13	258
7	100:0			491	0.48	267
8	100:0			505–520	<0.01	240–250
2	1:99[b]			518	0.62	261
9	10:90[c]		4:96[d]	520	0.23	258
10	33:67	22:78	22:78	520	0.07	257
11	6:94			521	0.35	258
12	8:92	4:96		506	0.44	257
13	27:73	16:84	18:82	523	0.12	254
14	100:0			510–515	<0.01	250–260
15	70:30[c]		66:24[d]	531	0.30	269

[a] The trans to cis ratio was determined by ^1H NMR measurement. [b] At 213 K. [c] At 223 K. [d] At 248 K. [e] Relative intensity is defined as the ratio of the fluorescence intensity of the compound in question to that of **1**.

Table II. Decay Times of Aromatic Anilides in MCH at 300 K

		lifetime		max
compd	conc (M)	in ps	in ns	count
1	2.5×10^{-4}	860		10000
	1.3×10^{-4}	860		10000
	3.0×10^{-5}	860		10000
2	3.2×10^{-4}	1650 (96%)	16.5 (4%)	10000
	9.5×10^{-5}	1660 (96%)	16.5 (4%)	10000
	2.6×10^{-5}	1650 (96%)	16.5 (4%)	10000
3	9.0×10^{-5}	770		10000
4	1.1×10^{-4}	550		1000
5	1.2×10^{-4}	990 (>99.9%)		10000
6	1.0×10^{-4}	680 (>99.9%)		1000
7	1.1×10^{-4}	860 (>99.8%)		10000
9	1.3×10^{-4}	1160 (98%)	16 (2%)	2000
10	2.6×10^{-4}	490		1000
11	1.2×10^{-4}	1300 (98%)	>6 (2%)	10000
12	1.6×10^{-4}	730		10000
13	1.6×10^{-4}	940		2000
15	1.5×10^{-4}	1520 (98%)	>36 (2%)	10000
16	2.0×10^{-4}	<30		10000

(8) Kagechika, H.; Himi, T.; Kawachi, E.; Shudo, K. *J. Med. Chem.* **1989**, *32*, 2292–2296.
(9) Toriumi, Y.; Kasuya, A.; Itai, A. *J. Org. Chem.* **1990**, *55*, 259–263.
(10) Itai, A.; Toriumi, Y.; Tomioka, N.; Kagechika, H.; Azumaya, I.; Shudo, K. *Tetrahedron Lett.* **1989**, *30*, 6177–6180.
(11) Azumaya, I., Kagechika H., Yamaguchi K., Shudo K. Unpublished results.

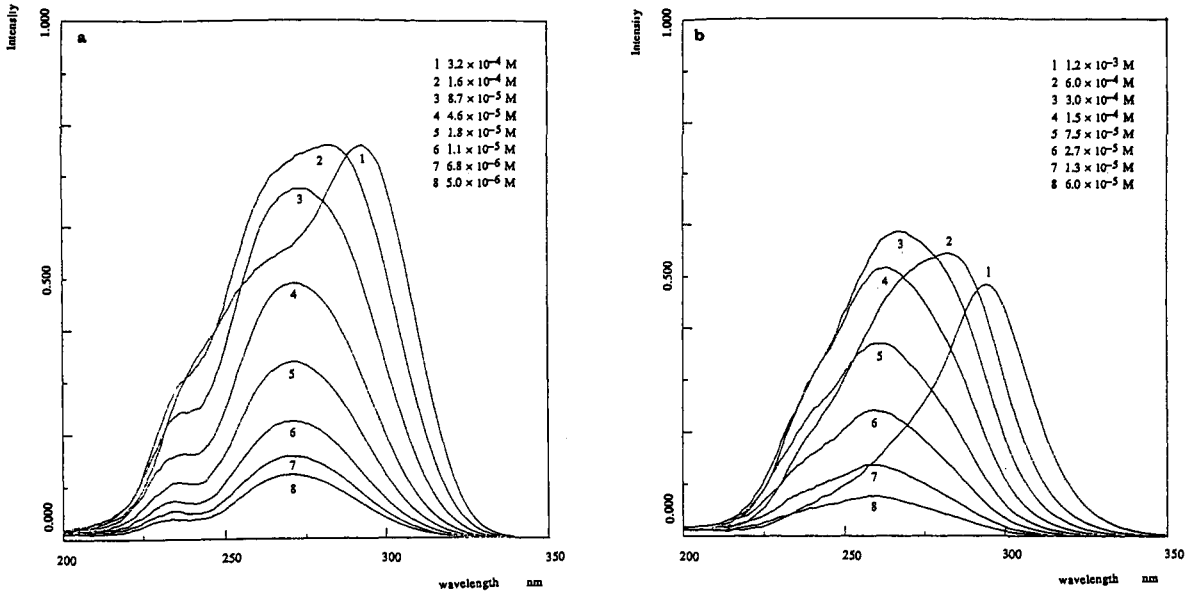

Figure 2. Excitation spectra of **1** ((a); λ_{em} 477 nm) and **2** ((b); λ_{em} 518 nm) at various concentrations in MCH.

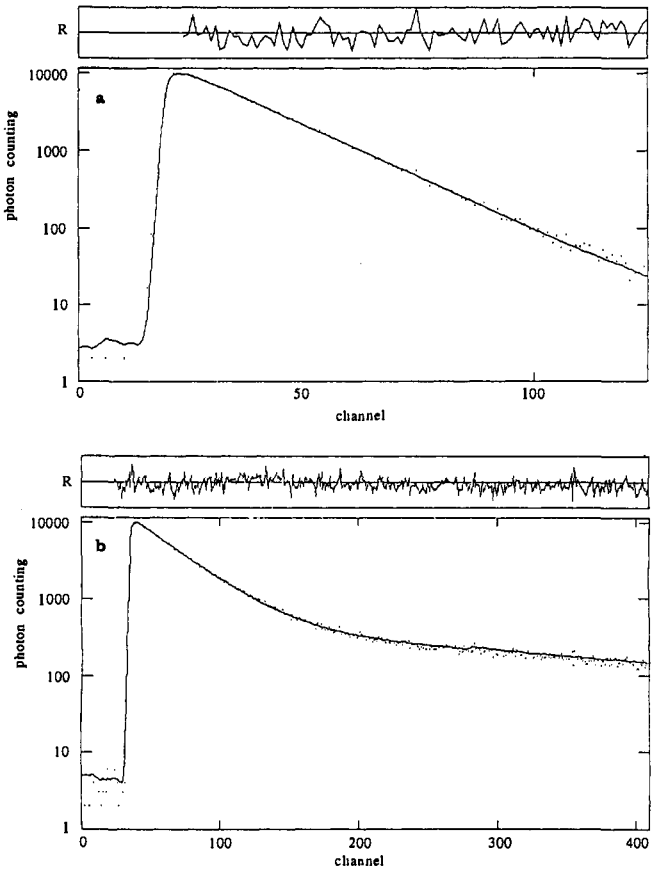

Figure 3. Fluorescence decay curves for F_2 emission of **1** (a); 1.3×10^{-4} M, detected at 477 nm) and **2** ((b); 9.5×10^{-5} M, detected at 518 nm) in MCH at 300 K. 53.5 ps per channel. Lines indicate the deconvolved decay functions. Single decay calculated for **1** with 860-ps decay constant and bimodel decay for **2** with 1650 ps (96%) and 16.5 ns (4%). Rise time (50 ps) was added to both decay functions.

F_2 emission of **1** originates from a single excited species. However, that of **2** has a minor decay component (16.5 ns). Further, the decay constants of both anilides did not change with concentration, which eliminated the possibility of the formation of dimers (Table II).

Ortho Substituent Effects on F_2 Emission. The decay dynamic studies indicated that the emitting mechanism for F_2 emissions is simpler than that proposed before and is common to both secondary and tertiary anilides. Contrary to the preference for

Chart I

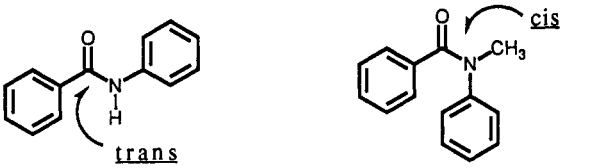

Benzanilide (1) N-Methylbenzanilide (2)

Chart II

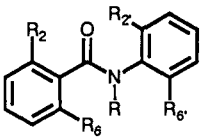

	R_2	R_6	$R_{2'}$	$R_{6'}$	R
3	Me	H	H	H	H
4	Me	Me	H	H	H
5	H	H	Me	H	H
6	H	H	Me	Me	H
7	Me	H	Me	H	H
8	Me	Me	Me	Me	H
9	Me	H	H	H	Me
10	Me	Me	H	H	Me
11	H	H	Me	H	Me
12	H	H	Me	Me	Me
13	Me	H	Me	H	Me
14	Me	Me	Me	Me	Me
15	H	H	H	$-CH_2CH_2-$	

trans-amide conformation of **1** both in the crystal and in solution, **2** exists in *cis*-amide conformation in the crystal and in solution (for example, 99% cis form in $CDCl_3$, Chart I).[8,12] Therefore, the excited conformations initially formed from **1** and **2** must be quite different from each other. In order to clarify the relationship between the conformation of the amide bond and F_2 emission, the

(12) Kashino, S.; Ito, K.; Haisa, M. *Bull. Chem. Soc. Jpn.* **1979**, *52*, 365.

Chart III

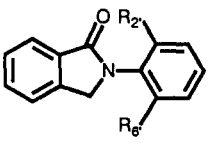

	$R_{2'}$	$R_{6'}$
16	H	H
17	Me	H
18	Me	Me

fluorescences of several aromatic anilides with methyl group(s) ortho to the amide bond were investigated (Chart II). Table I shows the trans to cis ratio and the maximum wavelengths and relative intensities of F_2 emissions of these anilides. Secondary anilides exist exclusively in trans form from X-ray crystallographic and NMR spectroscopic studies, except **4** (in $CDCl_3$), which has a minor (3%) cis conformer. The substitution of *o*-methyl group(s) resulted in decreased intensities of F_2 emissions. The fluorescence intensities of the compounds with two methyl groups on the same benzene ring (**4** and **6**) are only $^1/_{10}$ of that of **1**, and the compound with methyl groups at all ortho positions (**8**) essentially did not exhibit the F_2 emission. Similar features were seen in the tertiary anilides, although they exist in equilibrium between cis (major, except **14**) and trans forms in solution.

There are several significant tendencies apparent in the substituent effects.

First, the introduction of methyl group(s) ortho to the amide bond resulted in a decrease of the F_2 emissions. The steric hindrance of methyl group(s) caused loss of the planarity between the aromatic ring(s) and the amide bond (that is, Ar–N and Ar–CO), as was clearly apparent from their crystal structures.[11] Therefore, partial planarity of the molecule is necessary for F_2 emissions. Furthermore, the similarity in substituent effects between secondary and tertiary anilides suggested that similar emitting species would be formed from both types of anilides.

Second, the maximum wavelength values of the secondary anilides are within 477–490 nm except for the compounds with little fluorescence (**6** and **8**), and those of all the tertiary anilides are within 506–523 nm in spite of the wide range of the trans to cis ratios. Significantly, even the compounds that exist in equilibrium between trans and cis forms have only one maximum in their F_2 emissions. This is further confirmed by the studies of the decay dynamics (Table II). The single (over 98%) decay constants for fluorescence of **9–13** suggest that the same species must be formed from both trans and cis conformers in the excited states. Moreover, F_2 emissions of all the secondary anilides with acidic protons consist of only one component, as do those of the tertiary anilides, and so the participation of a proton-transfer mechanism is ruled out by our experiments.

Ring-Fixed Analogues of Benzanilides. The compounds made structurally rigid by introduction of a ring system provided further strict information about the emitting mechanisms of benzanilides. *N*-Benzoylindoline (**15**) is an analogue in which the Ar–N bond is fixed, and it exists in equilibrium between trans and cis forms (a ratio of 70:30 in $CDCl_3$ and 66:34 in CCl_4). Compound **15**

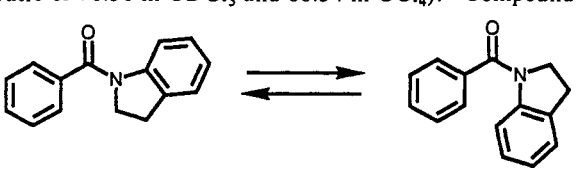

trans cis

N-Benzoylindoline (15)

also exhibited F_2 emission in MCH at room temperature, being very similar in this respect to the flexible benzanilides (Figure 4, Table I). The decay curve of F_2 emission of **15** is shown in

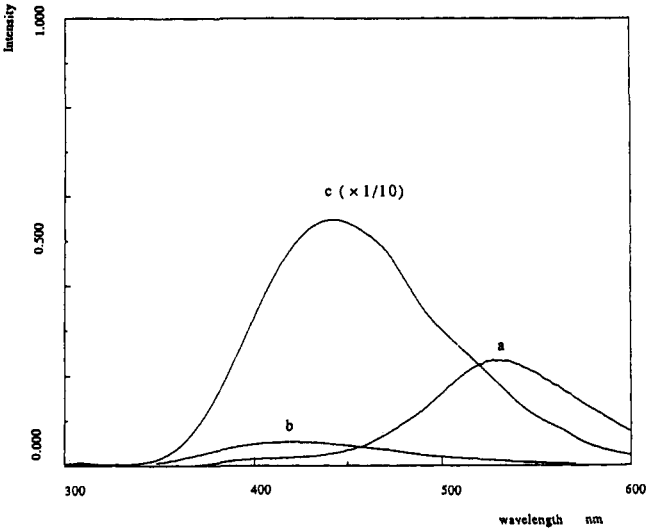

Figure 4. Fluorescence spectra of **15** in MCH ((a); 3.2×10^{-5} M) and *N*-phenylisoindolinone (**16**) in MCH ((b); 3.2×10^{-5} M) and in MeOH ((c); $\times\ ^1/_{10}$, 3.2×10^{-5} M) at 300 K. Each spectrum was obtained by excitation at the excitation maximum wavelength as shown in Table I for **15** and in Table III for **16**.

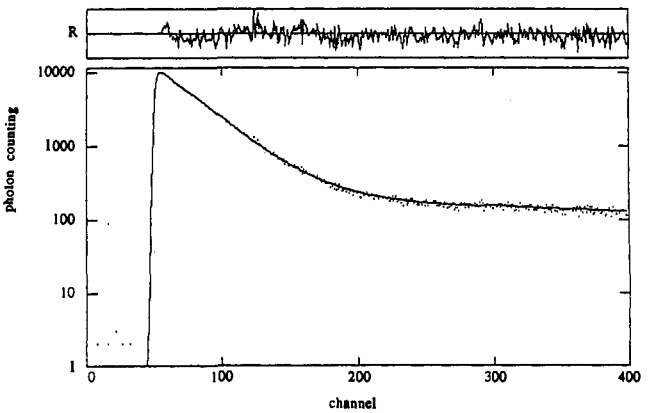

Figure 5. Fluorescence decay curve for F_2 emission of **15** (1.5×10^{-4} M, detected at 531 nm) in MCH at 300 K. 53.5 ps per channel. Decay time of the major component is calculated with 1520 ps (98%) and the minor (2%) with 36 ns.

Table III. F_2 Fluorescence Data of *N*-Phenylisoindolinone Derivatives (**16–18**) in MCH and in MeOH at 300 K

	F_2 emission in MCH			F_2 emission in MeOH		
compd	λ_{max} (nm)	rel intens[a]	excitation λ_{max} (nm)	λ_{max} (nm)	rel intens	excitation λ_{max} (nm)
1	477	1.00	271	none		
2	518	0.62	261	none		
16	422	0.08	310	442	5.58	264
17	444	0.02	272	468	0.48	266
18	none			447	0.62	264

[a] Relative intensity is defined as the ratio of the fluorescence intensity of the compound in question to that of **1** in MCH.

Figure 5. In this case again, the curve could be fitted with a single exponential (98%) in spite of the trans/cis equilibrium in the ground state.

On the other hand, *N*-phenylisoindolinones (**16–18**) are analogues in which the Ar–CO and amide bonds are fixed (Chart III). The emission spectra of three *N*-phenylisoindolinone derivatives in MCH and in methanol and their maximum wavelengths and intensities are compared with those of **1** and **2** (Table III). In contrast to the anilides discussed previously, **16** exhibits little F_2 emission in MCH and emits strongly in methanol at room temperature. In the case of *N*-phenylisoindolinones, substitution ortho to the amide group decreased the fluorescence intensity by 1 order of magnitude. Since the flexible anilides such as **1** and

Table IV. Physical Data for Aromatic Anilides (**1**–**18**)

compd	crystal form	recrystn, solvent	mp (°C)	formula	anal. calcd C	anal. calcd H	anal. calcd N	found C	found H	found N
1	colorless plates	MeOH	163–163.5	$C_{13}H_{11}NO$	79.17	5.67	7.10	78.98	5.63	7.06
2	colorless prisms	*n*-hexane	57	$C_{14}H_{13}NO$	79.59	6.20	6.63	79.29	6.17	6.46
3	colorless needles	MeOH	126.5–127	$C_{14}H_{13}NO$	79.59	6.20	6.63	79.62	6.25	6.63
4	colorless needles	AcOEt/*n*-hexane	137–138	$C_{15}H_{15}NO$	79.97	6.71	6.22	79.85	6.77	6.21
5	colorless needles	MeOH	142–142.5	$C_{14}H_{13}NO$	79.59	6.20	6.63	79.47	6.20	6.44
6	colorless needles	AcOEt/*n*-hexane	161.5–162	$C_{15}H_{15}NO$	79.97	6.71	6.22	79.96	6.68	6.17
7	colorless flakes	*n*-hexane	141–141.5	$C_{15}H_{15}NO$	79.97	6.71	6.22	79.96	6.78	6.30
8	colorless needles	*n*-hexane	198	$C_{17}H_{19}NO$	80.60	7.56	5.53	80.34	7.59	5.61
9	colorless prisms	*n*-hexane	47	$C_{15}H_{15}NO$	79.97	6.71	6.22	79.72	6.72	6.05
10	colorless prisms	*n*-hexane	66–67	$C_{16}H_{17}NO$	80.30	7.16	5.85	80.03	7.19	5.68
11	colorless pillars	*n*-hexane	64.5–65	$C_{15}H_{15}NO$	79.97	6.71	6.22	79.77	6.72	6.14
12	colorless leaves	*n*-hexane	120–121	$C_{16}H_{17}NO$	80.30	7.16	5.85	80.38	7.20	5.95
13	colorless prisms	*n*-hexane	60–61	$C_{16}H_{17}NO$	80.30	7.16	5.85	80.04	7.17	5.69
14	colorless needles	AcOEt/*n*-hexane	141.5–142	$C_{18}H_{19}NO$	80.86	7.92	5.24	80.59	7.87	5.24
15	colorless needles	AcOEt/*n*-hexane	121	$C_{15}H_{13}NO$	80.69	5.87	6.27	80.88	5.87	6.30
16	colorless leaves	AcOEt	162–163	$C_{14}H_{11}NO$	80.36	5.30	6.69	80.43	5.28	6.63
17	colorless prisms	AcOEt/*n*-hexane	97.5–98	$C_{15}H_{13}NO$	80.69	5.87	6.27	80.64	5.90	6.21
18	colorless prisms	AcOEt/*n*-hexane	124–124.5	$C_{16}H_{15}NO$	80.98	6.37	5.90	80.89	6.34	5.83

2 exhibit no fluorescence in methanol at room temperature, the fluorescence of **16** in methanol must represent a different type of emission. The maximum wavelength of the weak fluorescence of **16** in MCH is close to that in methanol. Therefore, the weak fluorescence of **16** in MCH is possibly the same type of fluorescence as in polar solvents and does not correspond to the fluroescence of the flexible anilides in nonpolar solvents. In fact, the addition of less than 1% w/w of methanol to MCH increased the fluorescence intensities of **16** strongly without causing any change of the maximum wavelength (data not shown). Thus, the fixation of Ar–CO and the amide bond caused the disappearance of the F_2 emission.

Structure of the Excited Species. As described previously, several aromatic amides exhibit anomalous dual peaks of fluorescence. F_1 emissions at normal wavelengths were difficult to characterize strictly, since they included some contribution from several photodegraded compounds. The fluorescence decay curves for F_1 emissions of **1** and **2** change their shapes with time under laser pulse irradiation (283.8 nm). However, in short-term measurements of decay dynamics, the F_1 emission of both compounds had very fast rise and short decay times (data not shown). These results indicated that the emitting species for F_1 emissions are close to the Franck–Condon structures. Considering the ground-state conformations, the species generated from **1** possesses the trans amide bond, while that from **2** possesses the cis amide bond.

In respect to F_2 emissions with large Stokes shifts, there are two types: one is due to flexible aromatic anilides such as **1** and **2** or *N*-benzoylindoline (**15**) in nonpolar solvents, and the other is due to rigid anilides (**16**–**18**) in polar solvents. The fluorescences of **1** and **2** in EPA reported by O'Connell et al. can be classified as the latter type of emission.[1] Considering the rigidity of the structure of the anilides (in the case of **16**) or the emitting conditions (the fluorescence of **1** in the solid state or in a rigid matrix at low temperature), this type of fluorescence is inferred to result from solvent reorientation or intersystem crossing. This suggestion is consistent with the decay dynamics of **16**, that is, the rapid rise time and short single decay constant (330 ps, in MeOH).

F_2 emissions in nonpolar solvents are observed in various flexible aromatic anilides, regardless of their conformational properties at the ground states. The decay dynamic studies show that there should be a single emitting mechanism if we ignore the very minor components (below 4%) in the cases of several tertiary anilides (not secondary anilides). The slow rise time (~50 ps for **1** and **2**, Figure 3) indicated that conformational changes might be involved. Significantly, even the anilides that exist in equilibrium between trans and cis conformers in solution exhibit emissions with a single maximum and a single decay constant, and therefore common stable excited species were derived from both Franck–Condon structures with trans and cis amide bonds. There are three flexible bonds in benzanilides that can change their conformations

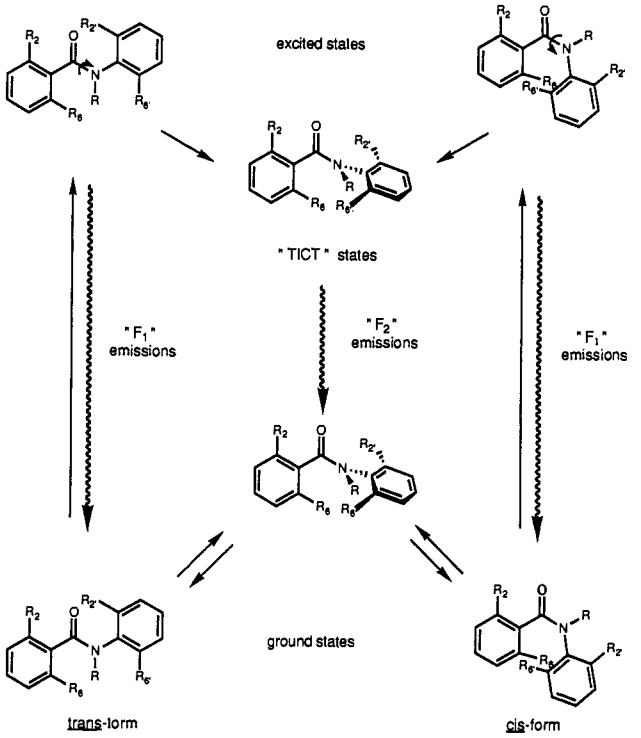

Figure 6. Mechanisms for F_1 and F_2 emissions of aromatic amides in nonpolar solvents.

in excited states; two Ar–amide bonds (Ar–CO and Ar–N) and the amide bond itself (N–CO). The anilides having two methyl groups on one of the benzene rings exhibit only weak fluorescences. In their crystal structures, and plausibly also the structures in solution, the Ar–CO and/or Ar–N bonds are significantly twisted for steric reasons. Since, however, the fluorescence intensities of these compounds were decreased, the twisting of either Ar–CO or Ar–N bonds is not favorable for the F_2 emissions. In the case of **16**, whose amide bond can not rotate, the absence of the F_2 emission in a nonpolar solvent indicates that rotation of the amide bond (N–CO) may be required for the F_2 emissions. Moreover, this would be compatible with the point that the observed F_2 emission of **15** was similar to those of other flexible anilides in respect to wavelength, intensity, and decay time. Thus, we concluded that F_2 emissions are generated from excited TICT species with twisted amide bonds (Figure 6). Generally, the stabilization of TICT structures can be interpreted in terms of charge separation. In order to elicit the charge separation efficiently in benzanilides, planarity must be acquired in Ar–CO and Ar–N. In the nonplanar structures of the anilides with *o*-methyl groups,

the separated charge could not be adequately stabilized by the aromatic ring(s). The energy levels of their twisted conformation in the ground states also must be higher, and therefore, their F_2 emissions were observed at a similar wavelength region.

In conclusion, the anomalous long-wavelength fluorescence of aromatic anilides in nonpolar solvents is emitted from a single species with a twisted amide bond (TICT states). In contrast to the poor stabilities of twisted conformations at the ground state, the twisted amide structures are greatly stabilized by charge separation arising from charge distribution to the aromatic rings.

Experimental Section

Materials. Melting points were determined by using a Yanagimoto hot-stage melting point apparatus and are uncorrected. Elemental analyses were carried out in the Microanalytical Laboratory, Faculty of Pharmaceutical Sciences, University of Tokyo and were within 0.3% of the theoretical values. ^{1}H NMR spectra were recorded on a JEOL GX 400-MHz NMR spectrometer.

MeOH (Dojin Luminasol) was purchased from Wako Pure Chemical Industries, Ltd. Methylcyclohexane (MCH, Dojin Spectrosol) was purified as follows. Aqueous saturated $KMnO_4$ (150 mL) was added to 750 mL of MCH, and the mixture was refluxed for several hours. The MCH layer was dried over $CaCl_2$. After decantation, the mixture was refluxed with 3 g of $LiAlH_4$ for several hours and then distilled under an Ar atmosphere. This MCH was dried over Na and stored. The effective purification of MCH was confirmed by the absence of fluorescence in the 300–700-nm region.

Benzanilide (**1**) is commercially available and was recrystallized twice from MeOH. The Me-substituted secondary amides (**3–8**) and *N*-benzoylindoline (**15**) were prepared by the condensations of the corresponding benzoyl chlorides and the corresponding anilines. *N*-Methylbenzanilide (**2**) and its *o*-Me-substituted derivatives (**9–14**) were prepared by N-methylation of corresp : ding secondary amides (NaH/DMF then MeI).

N-Phenylisoindolinone (**16**) and its derivatives (**17** and **18**) were prepared as follows.[13] *o*-Phthalaldehyde (4 mmol) was dissolved in 20 mL of AcOH, and the solution was heated at reflux. To this solution was added dropwise the corresponding aniline (10 mmol, large excess) in 2 mL of AcOH. After reflux for 20 min, the mixture was poured into water and extracted with AcOEt. The organic layer was washed with brine, 2 N HCl, brine, saturated $NaHCO_3$, and brine (twice) and dried over $MgSO_4$. The crude mixture was purified by silica gel column chromatography.

All the compounds for measurement were purified by recrystallization several times. Some of them were decolorized with activated carbon to give completely colorless crystals. The purities were certified by ^{1}H NMR, melting points, and elemental analysis. The physical data are listed in Table IV.

Apparatus. The time-correlated, single-photon counting system uses a synchronously pumped, cavity-dumped, Rhodamine 6G dye laser (Coherent 701) pumped by a mode-locked Nd:YAG laser (Coherent Antares 76-S) as an excitation source. The ultraviolet dye laser beam is frequency-doubled by using an angle-tuned β-BaB_2O_4 crystal (Tsukuba Asgal Co.) and is rotated to vertical polarization by a Babinet–Soliel compensator (Ohyoh Kohden). The laser beam is attenuated by suitable neutral density filters to ensure that the fluorescence count rate is always less than 1% of the cavity dumper frequency (generally 147 KHz).

Single fluorescence photons are detected by a Hamamatsu R2809U Michrochannel plate photomultiplier tube (MCPPMT) after polarization selection by a film polarizer obtained from Sigma Koki. The quartz collection optics are matched to those of the 0.2-m Ritsu monochromator (MC-20L) that is used for wavelength resolution.

The output of the MCPPMT is amplified by a Hewlett-Packard 8447D OPT001 dual power amplifier and conditioned by one of the four channels of a Tennelec TC 454 quad constant-fraction discriminator (CFD) whose output serves as the start signal for an Ortic 457 biased, time to pulse height converter (TAC). The stop signal comes from a Hamamatsu S1188-06 photodiode that monitors the output of the dye laser and is conditioned by another section of the CFD. This signal is delayed (Ortec DB463) such that signal appears on the screen of a Norand IT-5300 multichannel analyzer.

The instrument response function of the system, measured by using a diffuser, was found to be 105-ps full width at half-maximum and is independent of wavelength. The fluorescence decay curves were analyzed by a computer-simulated convolution.

Registry No. **1**, 93-98-1; **2**, 1934-92-5.

(13) Grigg, R.; Gunarante, H. Q. N.; Sridharan, V. *J. Chem. Soc., Chem. Commun.* **1985**, *17*, 1183–1184.